Tectonophysics, 50 (1978) 81—110

GLACIAL ISOSTASY AND RELATIVE SEA LEVEL: A GLOBAL FINITE ELEMENT MODEL

W.R. PELTIER, W.E. FARRELL and J.A. CLARK

Alfred P. Sloan Foundation Fellow, Department of Physics, University of Toronto, Toronto, Ont. M5S 1A7 (Canada)
Department of Materials Science and Mineral Engineering, University of California, Berkeley, Calif. 94720 (U.S.A.)
Department of Geological Sciences, Cornell University, Ithaca, N.Y. 14853 (U.S.A.)

(Accepted for publication April 17, 1978)

ABSTRACT

Peltier, W.R., Farrell, W.E. and Clark, J.A., 1978. Glacial isostasy and relative sea level: a global finite element model. In: M.N. Toksöz (Editor), Numerical Modeling in Geodynamics. Tectonophysics, 50: 81—110.

We review the subject of glacial isostatic adjustment and the structure of global models which have been developed to describe this phenomenon. Models of glacial isostasy have two basic ingredients: (1) an assumed deglaciation history, and (2) an assumed constitutive relation for the rheology of the planetary interior. Although both of these "functionals of the model" are imperfectly known, the parameters which are required to describe them are simultaneously constrained by observations of relative sea level. By comparing the model predictions of relative sea level for times subsequent to a major deglaciation event at a global distribution of sites, with the observed history of relative sea level at these sites, rather stringent bounds may be placed upon the model parameters.

INTRODUCTION

Observations of changes in the earth's shape produced by mass loads applied on its surface continue to provide a wealth of information concerning the physical properties of the interior. Such changes of shape are associated in general with both elastic and anelastic strains and with variations of the gravitational field. In order to deduce material properties from strain observations, assumptions must be adopted regarding the nature of the material of which the planet is composed. These assumptions are usually cast in the form of a constitutive relation connecting the stress τ and its time derivative $\dot{\tau}$ to the strain ϵ and its rate of change $\dot{\epsilon}$. The subject of the earth's rheology has always been one of the most controversial in geophysics.

Jeffreys has long maintained that an anelastic (lossy) rheology was important in seismology but only recently (Liu et al., 1976) have other seismologists become concerned with the effects that deviations from perfect

Hookean elasticity have on elastic wave propagation. At first glance this may seem surprising since the fact that the earth's mantle *is* anelastic (at least for deviatoric stresses which persist for thousands of years) has been appreciated for the better part of this century. Qualitatively this knowledge was based upon the recognition that the earth's shape continued to change *after* the last major deglaciation of the surface had been completed (a process which began about $2 \cdot 10^4$ years ago and ended ca $0.5 \cdot 10^4$). In formerly glaciated regions (e.g., Fennoscandia, Canada) old strandlines were found to be located hundreds of metres above present-day sea level. Detailed investigation of the stratigraphic record (in Fennoscandia) indicated a more or less exponential uplift of the surface of the solid earth with respect to local sea level. The rate of uplift has been a decreasing function of time since deglaciation, but is not yet complete.

With the advent of radiocarbon dating (e.g., Libby, 1952) and its subsequent application to the quantification of relative sea level data the detailed global history of the relaxation of shape following deglaciation began to emerge. Walcott (1972) has discussed these data (with emphasis on the Laurentide uplift) in detail and we may summarize their dominant features by noting that where the ice was thickest the land is now elevated above sea level, but only a short distance away from the two main centres of glaciation old beaches are drowned.

The generally exponential character of the uplift data is strongly suggestive of a simple relaxation process, and it is not surprising that they were initially interpreted in terms of a viscous fluid model of the interior (Haskell, 1935, 1936, 1937; Vening Meinesz, 1937; Niskanen, 1948). This model is, of course, the antithesis rheologically of the Hookean elastic model which, at that time, had been found to accord well with seismic observation. In order to fit the observed relaxation times (ca 10^3 years) fluid models with molecular viscosities on the order of 10^{22} poise (cgs) were required. This magic number has existed in the literature for over 40 years. Our recent attempts to quantify the extent of our ignorance of this parameter have been motivated by several concerns. In the first instance we would like to know, as accurately as possible, how the viscosity varies with radius in the mantle. Secondly, and more fundamentally, we wish to understand the microphysics of the process(es) by which mantle material "creeps" in response to an applied stress. Finally, using "improved" viscosity models we wish to study the breakup and disintegration of the Pleistocene ice caps and the impact which this event had upon the rotation of the earth. These facets of the problem are of fundamental importance to climatology. In the remainder of this introduction we will discuss the first two questions in turn.

The transport coefficient for momentum, ν, (i.e., the viscosity) plays a decisive role in geodynamic models of long timescale processes in the planetary interior. For example, since the Rayleigh number for thermal convection, Ra, is such that $Ra \propto \nu^{-1}$, the higher the viscosity the less vigorous will be the convection forced by a given superadiabatic temperature gradient. As

ν increases the efficiency of convective heat transport decreases; thus the magnitude of this parameter has a direct impact upon the thermal history of the earth. If the viscosity were to increase sufficiently rapidly with depth then convection in the lower mantle would be inhibited. If one associates the downgoing slabs of plate tectonic theory with the descending limbs of cold thermal boundary layers of the global convective circulation, then seismic focal mechanism data (Isacks and Molnar, 1971) suggest that the slab encounters some resistance to continued vertical motion near a depth of 650 km. This resistance has been attributed by some to a rapid increase of viscosity, assumed to be a consequence of the spinel—post-spinel phase change. In order that convection be effectively inhibited from penetrating this hypothesized boundary an increase in viscosity of several orders of magnitude is required. Such a large viscosity increase at this depth ought to be detectable through careful analysis of the relaxation data.

Until rather recently (Cathles, 1975; Peltier, 1974; Peltier and Andrews, 1976) it has generally been believed that the isostatic adjustment data did in fact *require* a rapid increase of viscosity with depth. The strongest evidence was presented by McConnell (1968) through an analysis of the Fennoscandia data. In order to obtain resolution for lower mantle viscosity, however, his analysis made use of an inferred relaxation time for the $n = 2$ harmonic of the gravitational field of approximately 10^{13} sec. This inference was based upon two assumptions: (1) that the earth had a "genuine" non-hydrostatic equatorial bulge, and (2) that this bulge was itself caused by Pleistocene glaciation. The relaxation time was then deduced by interpreting historical changes in the length of the day as being a consequence of the collapse of the bulge. This interpretation led McConnell to suggest lower mantle viscosities on the order of 10^{25} poise.

McKenzie (1966) arrived at a similar conclusion which was again based upon an interpretation of the non-hydrostatic equatorial bulge. He assumed, as had been suggested in Munk and Macdonald (1960), that the excess bulge was a relic from a time when the earth was spinning faster than at present and its continued existence then suggested that the viscosity of the deep mantle must be extreme. This conclusion, and likewise McConnell's, was completely undermined by Goldreich and Toomre (1969) who showed that the non-hydrostatic bulge upon which both arguments were based was only an artifact of the spherical harmonic analysis in terms of which its existence had originally been suggested. The relaxation data from Fennoscandia did not, in themselves, suggest or even support the existence of a steep viscosity gradient in the upper mantle. McConnell (1968) elected not to fit his own long wavelength relaxation data, giving arguments as to why these should be inaccurate.

More recently Parsons (1972) has shown through a "resolving power" analysis of McConnell's original data that these are simply incapable of providing any information on the viscosity of the mantle at depths in excess of about 600 km. This is due to the relatively small horizontal scale of the Fen-

noscandian rebound. The usefulness of these data therefore fades at just those depths at which we become most interested. It is the existence of new data associated with the recovery of the larger scale Laurentide region (most of Canada) which has encouraged our re-examination of the isostatic adjustment process in an attempt to test the plate resistance hypothesis. Since the dominant wave number of the relaxation in this region corresponds to spherical harmonic degrees of the order of $n \cong 5$ whereas the Fennoscandia data provide information on $n \cong 16$ we expect that the Canadian data are potentially able ro resolve viscosity variations throughout the entire mantle. On the basis of analyses of this data Cathles (1975) and Peltier and Andrews (1976) have shown that the observed recovery is incompatible with a viscosity profile which is a rapidly increasing function of depth and in fact both studies found that a uniform mantle viscosity with $\nu \cong 10^{22}$ poise gives a reasonable fit to the data. These interpretations were based, however, upon theoretical models which were not consistent gravitationally in that the surface of the ocean was not constrained to remain an equipotential surface during and following deglaciation. One of the main purposes of the present paper is to summarize recent work which has remedied this defect and in the process has reinforced the original conclusions.

Although the inference of viscosity from relaxation data does not *require* a microphysical model of the creep mechanism, it is nevertheless true that the number which one assigns to this parameter may exhibit a dependence upon the model assumed. From a continuum mechanical point of view, microphysical models may be classified as either Newtonian or non-Newtonian. In the former case the relation between the stress and strain-rate tensors is linear and the coefficient of proportionality is the Newtonian viscosity, whereas in the latter the relation is non-linear and the effective viscosity is therefore stress dependent. When a Newtonian constitutive relation is employed then one is implicitly assuming that the creep mechanism is Herring—Nabarro or Coble or some other mechanism which leads to a linear relation between τ and $\dot{\epsilon}$. For the Herring—Nabarro mechanism (Herring, 1950) the equivalent Newtonian viscosity ν_N is:

$$\nu_N = (kTa^2/\alpha_0 D_0 \Omega) \exp[(E + pV_a)/kT] \tag{1}$$

where k is Boltzmann's constant, T the absolute temperature, V_a the activation volume, a the grain radius (assumed constant), E the activation energy for self diffusion of the rate limiting species, p the pressure, Ω the atomic volume, and α_0 (≈ 5) is a dimensionless constant. The constitutive relation is then $\tau = \nu_N \dot{\epsilon}$. All microphysical mechanisms lead to expressions for the viscosity which are explicit functions of the thermodynamic coordinates. If we knew the way in which these coordinates varied with depth and correct values for the other parameters then we could deduce the viscosity depth profile directly (e.g., Sammis et al., 1977). Such, however, is unfortunately not the case. In interpreting the postglacial relaxation data what we are obliged to do is to suppress the explicit dependence of ν upon p, T, etc. and to

include such dependence in the model through an assumed depth dependence. We then attempt to find the $\nu(r)$ which best fits the observations.

The existence of microphysical mechanisms which lead to linear macroscopic constitutive relations has provided some solace to those who would construct mathematical models of the stress relaxation associated with isostatic adjustment or of the mantle convective circulation. This is clearly due to the fact that a linear constitutive relation is easier to manage than a nonlinear one. However, recent experimental evidence (Ashby, 1972; Stocker and Ashby, 1973; Post and Griggs, 1973; Kohlstedt and Goetze, 1974) on the creep of mantle material (mostly olivine single crystals) suggests strongly that the rate limiting process is *not* linear. The experimental data rather suggests a power law creep equation with a stress exponent $m \approx 3$. Weertman and Weertman (1975) have reviewed the interpretation of these data and their implications in some detail.

A general form of the power law creep equation with $m = 3$ may be written as:

$$\dot{\epsilon} = \gamma(D/b^2)(\mu\Omega/kT)(\sigma/\mu)^3 \tag{2}$$

where the self diffusion coefficient D for the rate limiting species is

$$D = D_0 \exp\left[\frac{-\mathrm{E} - pV_a}{kT}\right]$$

in which γ is a dimensionless constant, b is the length of the Burghers vector of the dislocation, and where μ is the elastic shear modulus. The remaining symbols are the same as in eq. 1. We may invert eq. 2 to write $\tau = \nu_{NN}\dot{\epsilon}$ where ν_{NN} is now a function of stress so that the constitutive relation is nonlinear. The laboratory data which suggest eq. 2 are, of necessity, taken for creep rates which are enormously in excess of those which are associated either with rebound or with convection (i.e., 10^{-6} s^{-1} as opposed to 10^{-16} s^{-1}). The interpretation therefore requires a huge extrapolation of the actual data.

In the models of isostatic adjustment described below we *assume* that the stress—strain relation is Newtonian. In fact we employ a model earth which is a simple linearly visco-elastic (Maxwell) solid. What we seek to accomplish is a direct test of this constitutive relation, and the test demands the resolution of two distinct questions. Firstly, is it possible with such a model to fit the observed relative sea level data? If the answer to this question is an unambiguous "yes" then we must furthermore attempt to understand the extent to which non-Newtonian models are capable of providing similar accord with the data. Here we shall only be concerned with an attempt to answer the first question. Brennan (1974) and Crough (1977) have made initial attempts to address the second but much further work remains to be done in this area.

The data which we must interpret concern the location with respect to present day sea level of raised or submerged beaches, the age of which may be determined by application of ^{14}C dating methods. These histories of rela-

tive sea level are a record of the manner in which the earth and its ice sheets and oceans responded to the cataclysmic redistribution of surface mass associated with the last major climatic change. They are the "seismograms" of ultra-low frequency geodynamics and — to continue the analogy — the deglaciation event was the equivalent "earthquake". In order to interpret these relative sea level data we must be able to construct the "synthetic seismograms" of the process. That is, given a certain model of deglaciation and a rheological model of the earth we need a theory which can predict relative sea level as a function of time everywhere where continent and ocean meet. The solution of this forward problem and of the inverse *problems* related to it (Peltier, 1976) are now practicable and the theoretical model and initial results of its application are reviewed below.

THE IMPULSE RESPONSE OF A MAXWELL EARTH

The simplest rheological model in terms of which *both* the instantaneous elastic and the long time scale viscous reactions to surface loading may be accommodated is that for a Maxwell solid. The stress—strain relation for a Maxwell medium is (Malvern, 1969):

$$\dot{\tau}_{kl} + \frac{\mu}{\nu}(\tau_{kl} - \tfrac{1}{3}\tau_{kk}\delta_{kl}) = 2\mu\dot{e}_{kl} + \lambda\dot{e}_{kk}\delta_{kl} \tag{3}$$

where τ_{kl} and e_{kl} are respectively the tensors for stress and strain and where μ and λ are the conventional Lamé parameters of elasticity. The dot denotes time differentiation. The first thing to note about eq. 3 is that it is linear. We can understand its physical content most simply by representing both tensors in terms of their Laplace transforms, i.e., by using the transform pair:

$$\tilde{\tau}_{kl} = \int_0^\infty dt\, e^{-st}\, \tau_{kl}$$

$$\tau_{kl} = \frac{1}{2\pi i}\int_B ds\, e^{st}\, \tilde{\tau}_{kl} \tag{4}$$

and similarly for e_{kl}. In eq. 4 B is the Bromwich path. In the Laplace transform domain of the imaginary frequency s eq. 3 becomes:

$$\tilde{\tau}_{kl} = \lambda(s)\, \tilde{e}_{kk}\delta_{kl} + 2\mu(s)\, \tilde{e}_{kl} \tag{5}$$

where $\lambda(s)$ and $\mu(s)$ are the following "compliances":

$$\lambda(s) = \frac{\lambda \cdot s + \mu K/\nu}{s + \mu/\nu} : \mu(s) = \frac{\mu \cdot s}{s + \mu/\nu} \tag{6}$$

where $K = \lambda + \frac{2}{3}\mu$ is independent of s. We note that in terms of these compli-

ances the Laplace transformed constitutive relation has the same *form* as that for a Hookean elastic solid.

We can see clearly the way this material "works" by considering the two separate limits $s \to \infty$ and $s \to 0$ which correspond to short time scale and long time scale behaviour respectively (via the Tauberian theorems). Note that both s and μ/ν have the dimensions of inverse time. The "Maxwell time" is just $T_m = \nu/\mu$. For $t << T_m$ (i.e., $s >> \mu/\nu$) we see from eq. 6 that $\lambda(s) \to \lambda$ and $\mu(s) \to \mu$ so that the material behaves as a Hookean elastic solid. In the opposite limit, $t >> T_m$, $\lambda(s) \to K$, $\mu(s) \to 2\nu s$ and in the time domain the stress—strain relation becomes

$$\tau_{kl} = Ke_{kk}\delta_{kl} + 2\nu\dot{e}_{kl} \tag{7}$$

which is just that for an incompressible Newtonian fluid. The Maxwell solid is therefore "initially" elastic in its response to an applied stress and "finally" Newtonian viscous. The transition time between these asymptotic extremes is $T_m = 0$ (10^2 years). Thus for times in excess of a few hundred years after unloading the Maxwell earth behaves as a Newtonian viscous fluid. The constitutive relation for a standard linear solid (the most general visco-elastic model) differs from eq. 3 only in the addition of terms involving e_{kl} itself. The addition of such terms introduces a second viscosity coefficient associated with the Kelvin—Voigt element and there is thus dissipation associated with the short time scale response. Such rheologies are currently being investigated in the course of constructing earth models which have seismic velocity dispersion due to anelasticity (Liu et al., 1976; Kanamori and Anderson, 1977).

To solve the surface loading problem for Maxwell models we make use of the "Correspondence Principle" first described by Biot (1954) and Lee (1955). The principle is very simple to apply since it amounts to nothing more than a direct exploitation of the analogy between the visco-elastic constitutive relation (5) and that for a Hookean elastic solid. What we do is to solve an equivalent elastic problem many times for different values of the Laplace transform variable s to construct the "s-spectrum" of the solution. We then invert the spectrum to obtain its time domain form (Peltier, 1974).

The appropriate Laplace transformed and linearized field equations, respectively for the balance of momentum and for the perturbation of the gravitational potential are:

$$\underline{\nabla} \cdot \underline{\underline{\tilde{\tau}}} - \underline{\nabla}(\rho g \underline{u} \cdot \underline{e}_r) - \rho \underline{\nabla}\tilde{\phi} + g\underline{\nabla} \cdot (\rho \underline{\tilde{u}})\underline{e}_r = 0 \tag{8a}$$

$$\nabla^2\tilde{\phi} = -4\pi G \underline{\nabla} \cdot (\rho \underline{\tilde{u}}) \tag{8b}$$

where $\rho = \rho(r)$ is the density field in the basic hydrostatic equilibrium configuration, $g = g(r)$ is gravitational acceleration in the same state, $\underline{u}$ is the displacement field, ϕ the perturbation of the ambient gravitational potential, and G the gravitational constant. In eq. 8 $\underline{\nabla} \cdot (\rho \underline{u}) = \rho'$ has been substituted from the time integral of the continuity equation. The tilda, as before, repre-

sents implicit dependence upon the Laplace transform variable s. Thus $\underline{\underline{\tau}}$ in eq. 8 is given by eq. 5. In eq. 8a the inertial force is suppressed because of the long time scale of the phenomenon in which we are interested. The second and fourth terms on the left hand side of eq. 8a require additional explanation. That the second term should appear in the elastic limit is well known (Love, 1911) and arises due to the existence of the hydrostatic prestress in the compressible medium. Since the ambient state is assumed hydrostatic $\partial p/\partial r = -\rho g$ where $p(r)$ is the ambient pressure field. In an elastic displacement the material effectively transports its prestress with it. The fourth term in eq. 8a is the buoyancy force, since $\rho' = \underline{\nabla} \cdot (\rho \underline{u})$ from the continuity equation. If the background density field is adiabatic then this term should not appear in the viscous limit. It has been discussed by Cathles (1975) and by Peltier (1978).

We seek solutions to eq. 8 for $(\underline{u}, \phi)$ when the earth is deformed by gravitational interaction with a point mass load which is placed on its surface at $t = 0$ and instantaneously removed. If the physical properties of the interior $(\rho, \mu, \lambda, \nu)$ are functions of radius only then the response will be a function or (r, θ, s) only, where θ is the angular distance from the load. We may then expand $\underline{u}$ and ϕ as:

$$\tilde{\underline{u}} = \sum_{n=0}^{\infty} \left(U_n(r, s) P_n(\cos\theta) \underline{e}_r + V_n(r, s) \frac{\partial P_n(\cos\theta)}{\partial \theta} \underline{e}_\theta \right)$$

$$\tilde{\phi} = \sum_{n=0}^{\infty} \phi_n(r, s) P_n(\cos\theta) \tag{9}$$

where $U_n(r, s)$, $V_n(r, s)$, $\phi_n(r, s)$ are spectral amplitudes for the harmonic disturbance of degree n and imaginary frequency s. Subject to appropriate boundary conditions on $r = a$ (the earth's surface) we may construct solutions for the spectral amplitudes in the form (Peltier, 1974):

$$\begin{vmatrix} U_n \\ V_n \\ \phi_{1,n} \end{vmatrix} = \phi_{2,n}(r) \cdot \begin{vmatrix} h_n(r, s)/g \\ l_n(r, s)/g \\ k_n(r, s) \end{vmatrix} \tag{10}$$

where $\phi_n = \phi_{1,n} + \phi_{2,n}$ and $\phi_{2,n}$ is the perturbation of the gravitational potential due to the mass of the applied load. $\phi_{2,n}$ is independent of s since the applied load is assumed to have a $\delta(t)$ time dependence. The triplet of dimensionless scalars (h_n, l_n, k_n) thus constitute the non-dimensional spectral form of the impulse response of the system. They are the visco-elastic analogues of the so-called surface load "Love Numbers" of elasticity. Only the doublet (h_n, k_n) concerns us here. An example of the spectral surface $h_n(a, s)$ is shown in Fig. 1 for an earth model in which $\nu = \infty$ to a depth of 112.5 km (the lithosphere), $\nu = 10^{22}$ poise between the base of the lithosphere and the

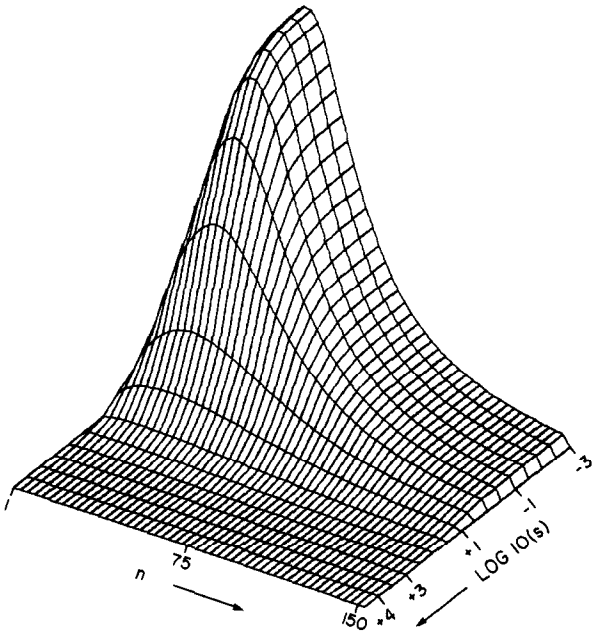

Fig. 1. The spectral surface $h_n^V(a, s)$ for the earth model described in the text which has a "lithosphere" of thickness $T = 112.5$ km at the surface $r = a$. Note that for large $n \gtrsim 150 h_n^V \equiv 0$ indicating that such short wavelength disturbances do *not* relax viscously. They are entirely supported by the lithosphere in which $\nu = \infty$.

core mantle boundary, and $\nu = 0$ throughout the core. The elastic structure of the model is "Gutenburg-Bullen A". In Fig. 1 we have in fact plotted $h_n^V(a, s) = h_n(a, s) - h_n^E$ where h_n^E is the large s elastic asymptote for each value of n (Peltier, 1974). In Fig. 1 it is clear that an additional asymptote exists for these spectra at small s.

It may be shown directly that these spectra have *exact* normal mode expansions of the form (Peltier, 1976):

$$h_n(s) = \sum_j \frac{r_j^n}{s + s_j^n} + h_n^E \tag{11}$$

where the s_j^n are a set of poles (a different set for each n) which lie on the negative real axis in the complex s-plane. The r_j^n are simply the residues at these poles and thus measure the extent to which a given normal mode is excited by the point forcing. A relaxation diagram showing the location of these poles for all n is shown in Fig. 2. The poles on this plot are marked with labels *MO*, *CO*, etc. which denote specific families which are distinguished from one another (Peltier, 1976) by the way in which the shear energy within them is distributed in radius. For example in *CO*, the fundamental core mode, the shear energy maximizes near the core—mantle boundary.

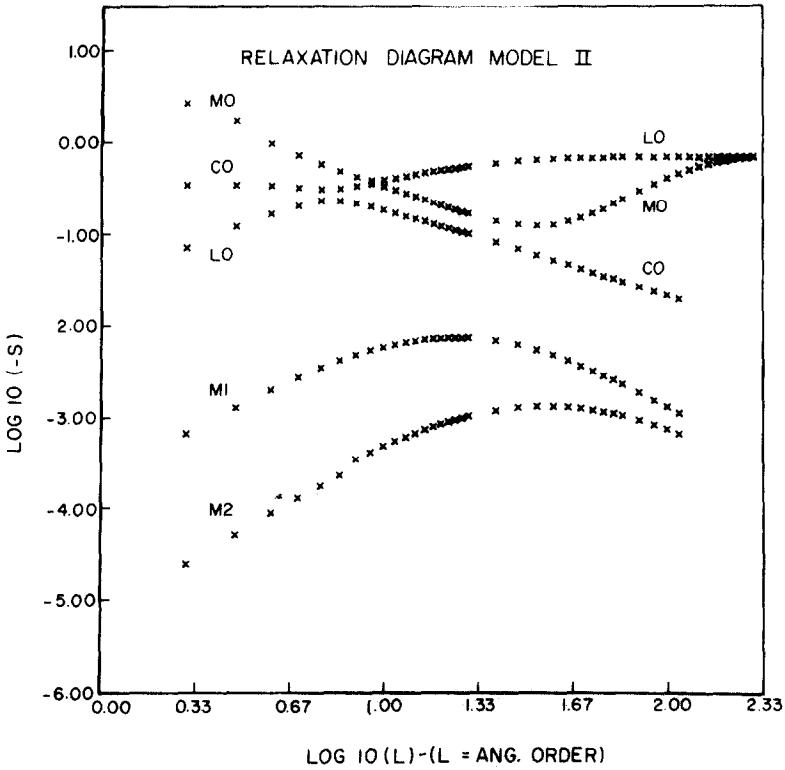

Fig. 2. Relaxation diagram for the earth model with lithosphere showing the location and multiplicity of the poles in the relaxation spectrum for each value of n. The ordinate is the logarithm of the inverse relaxation time and the relaxation times are all non-dimensionalized with a time scale of 10^3 years.

The above normal mode expansions of $h_n(s)$ and $k_n(s)$ have simple time domain representations:

$$h_n(t) = \sum_j r_j^n e^{-s_j^n t} + h_n^E \delta(t) \tag{12}$$

Remember that these are the non-dimensional spectral amplitudes for a temporally impulsive surface mass loading. If the load were allowed to remain on the surface for all $t > 0$ the time dependent harmonic amplitudes which result are obtained from the above simply by convolution with a Heaviside step function to give a form which has been previously labelled (Peltier and Andrews, 1976):

$$h_n^H(t) = \sum_j \frac{r_j^n}{s_j^n} (1 - e^{-s_j^n t}) + h_n^E = h_n^{H,V}(t) + h_n^E \tag{13}$$

Now notice that in the limit $t \to \infty$ these amplitudes are just:

$$\lim_{t \to \infty} h_n^H(t) = \sum_j \frac{r_j^n}{s_j^n} + h_n^E = \lim_{s \to 0} h_n(s) \tag{14}$$

The mechanism of isostatic compensation is thus clearly described in terms of these time dependent harmonic amplitudes. The number $\Sigma_j(r_j^n/s_j^n)$ for each wavenumber n describes the viscous contribution to the final isostatically adjusted amplitude of the disturbance. An example of the $h_n^{H,V}(t)$ is illustrated in Fig. 3 for the previous earth model.

We may obtain Green functions for various signatures of the response in terms of the Love Numbers h_n and k_n by summing infinite series as described by Farrell (1972) for the elastic problem and by Peltier (1974) for the viscoelastic equivalent. For example, the space and time dependent radial displacement of the original spherical surface is (for a unit applied point mass load):

$$u_r^H(\theta, t) = \frac{a}{M_e} \sum_{n=0}^{\infty} h_n^H(t) P_n(\cos\theta) \tag{15}$$

and the gravity anomaly on the deformed surface is:

$$\Delta g^H(\theta, t) = \frac{g}{M_e} \sum_{n=0}^{\infty} [n - 2h_n^H(t) - (n+1)k_n^H(t)] P_n(\cos\theta) \tag{16}$$

whereas the perturbation of the ambient gravitational potential on the deformed surface is (M_e is the mass of the earth):

$$\phi^H(\theta, t) = \frac{ag}{M_e} \sum_{n=0}^{\infty} (1 + k_n^H - h_n^H) P_n(\cos\theta) \tag{17}$$

We will see in the next section that the latter is particularly important insofar as the prediction of relative sea level is concerned. Here we illustrate the Green functions in Fig. 4 where $u_r^{H,V}(\theta, t)$ for the previous earth model is shown. This function has been normalized by multiplication with "$a\theta$" to remove the geometric singularity and $u_r^{H,V}(\theta, t) = u_r^H(\theta, t) - u_r^E(\theta, t)$. If a lithosphere is not included in the model then $u_r^{H,V}$ is singular in the limit $t \to \infty$ (Peltier, 1978) so that without a lithosphere is not possible to calculate the set of isostatic Green functions which obtain in this limit. This singularity is simply a consequence of the physical fact that if the planet is everywhere viscous then a point mass placed on its surface will eventually sink to the planet's centre since this is the only position at which it will feel no net force. Since the gravity anomalies which we observe are associated with the extent of isostatic disequilibrium, in order to predict them with the model we require the infinite time Green function and thus need a lithosphere.

Given the Green functions determined as described above we may deduce the response of the earth model to the gravitational forcing associated with a surface load which has an arbitrary space–time dependence. Since the model is linear the solution under such circumstances may be obtained simply by invoking the principle of superposition. If we had a set of data which *exactly*

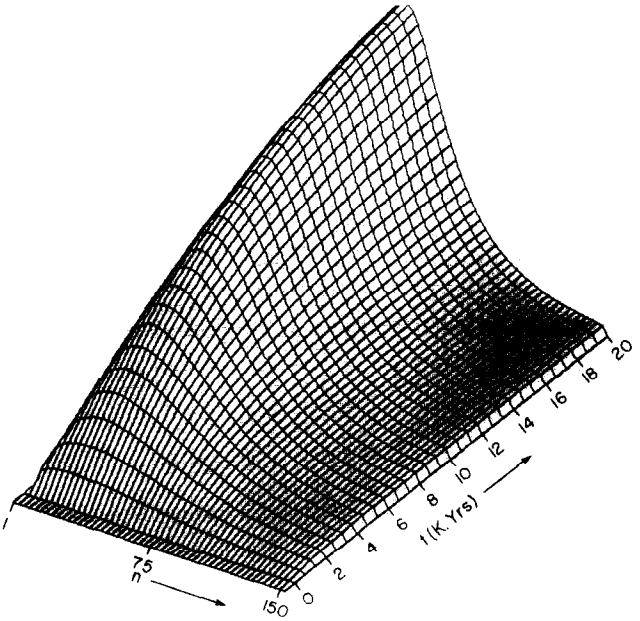

Fig. 3. The relaxation surface $h_n^{HV}(a, t)$ for the earth model with lithosphere. Note that for $h_n \gtrsim 150 h_n^{HV}(a, t) \equiv 0$ so that sufficiently short wavelengths show no viscous relaxation. This was pointed out previously in connection with Fig. 1.

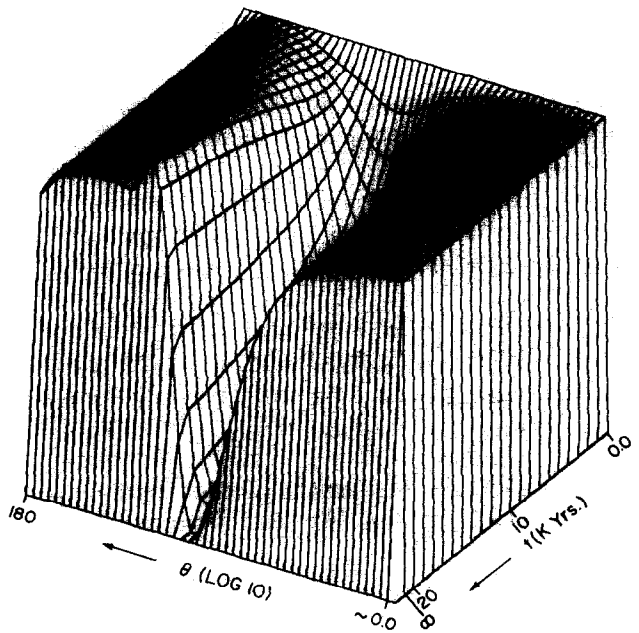

Fig. 4. Viscous part of the radial displacement Green function $u_r^{HV}(\theta, t)$ for the earth model with lithosphere. The effect of the geometric singularity at $\theta = 0$ has been removed for the purpose of illustration by multiplication with "$a\theta$".

recorded the time dependence of the variation of local radius $\Delta R(\theta, \phi, t)$ as a function of position on the surface (θ, ϕ) then the model prediction of this data would take the form:

$$\Delta R(\theta, \phi, t) = \iint d\Omega' \int_0^t dt' \, u_r(\theta/\theta', \phi/\phi', t/t') L(\theta', \phi', t') \tag{18}$$

where u_r is the kernel in the convolution integral, $d\Omega'$ the element of surface area, and L is the surface mass load functional which has the dimensions of mass per unit area (i.e., density × thickness). If the redistribution of mass on the surface takes place at a single instant of time then we can do the temporal part of the three variable convolution in eq. 18 analytically. The result is simply (Peltier and Andrews, 1976):

$$\Delta R^H(\theta, \phi, t) = \iint d\Omega' \, u_r^H(\theta/\theta', \phi/\phi', t) L(\theta', \phi') \tag{19}$$

For a more general history of load redistribution we may obtain the solution by the superposition of forms like eq. 19 which are appropriately weighted and phased in time.

Inspection of eq. 19 reveals two fundamental difficulties in applying the theory both of which are associated with L. Since the surface load must conserve mass and since it consists of two distinct parts associated respectively with the melting of the ice and the simultaneous filling of the ocean basins we may expand L as:

$$L = \rho_I L_I(\theta, \phi, t) + \rho_W L_O(\theta, \phi, t) \tag{20}$$

where ρ_I and ρ_W are the density of ice and water respectively, and L_I and L_O are the corresponding thickness. We assume that the hydrological cycle is closed so that mass conservation demands:

$$\int d\Omega \, \rho_W L_O = M_O = -\int d\Omega \, \rho_I L_I = -M_I \tag{21}$$

which is clearly an integral constraint on the model load history. Given $M_I(t)$, the time dependent mass flux to the ocean basins (assumed negative for melting), we can convert M_O to a uniform *equivalent* time dependent rise of sea level which we call:

$$S_{EUS} = \frac{M_O(t)}{\rho_W \cdot A_O} \tag{22}$$

where A_O is the surface area of the world ocean which we may assume to a good approximation is not affected by the sea level rise. Now S_{EUS} is an equivalent rise of sea level and we do not wish to suggest by eq. 22 that the sea level rise is uniform everywhere over the global ocean. Clearly it could not be uniform for then the "new" ocean would have a surface which was not everywhere an equipotential. *Given* $M_I = -M_O$ we must in fact determine

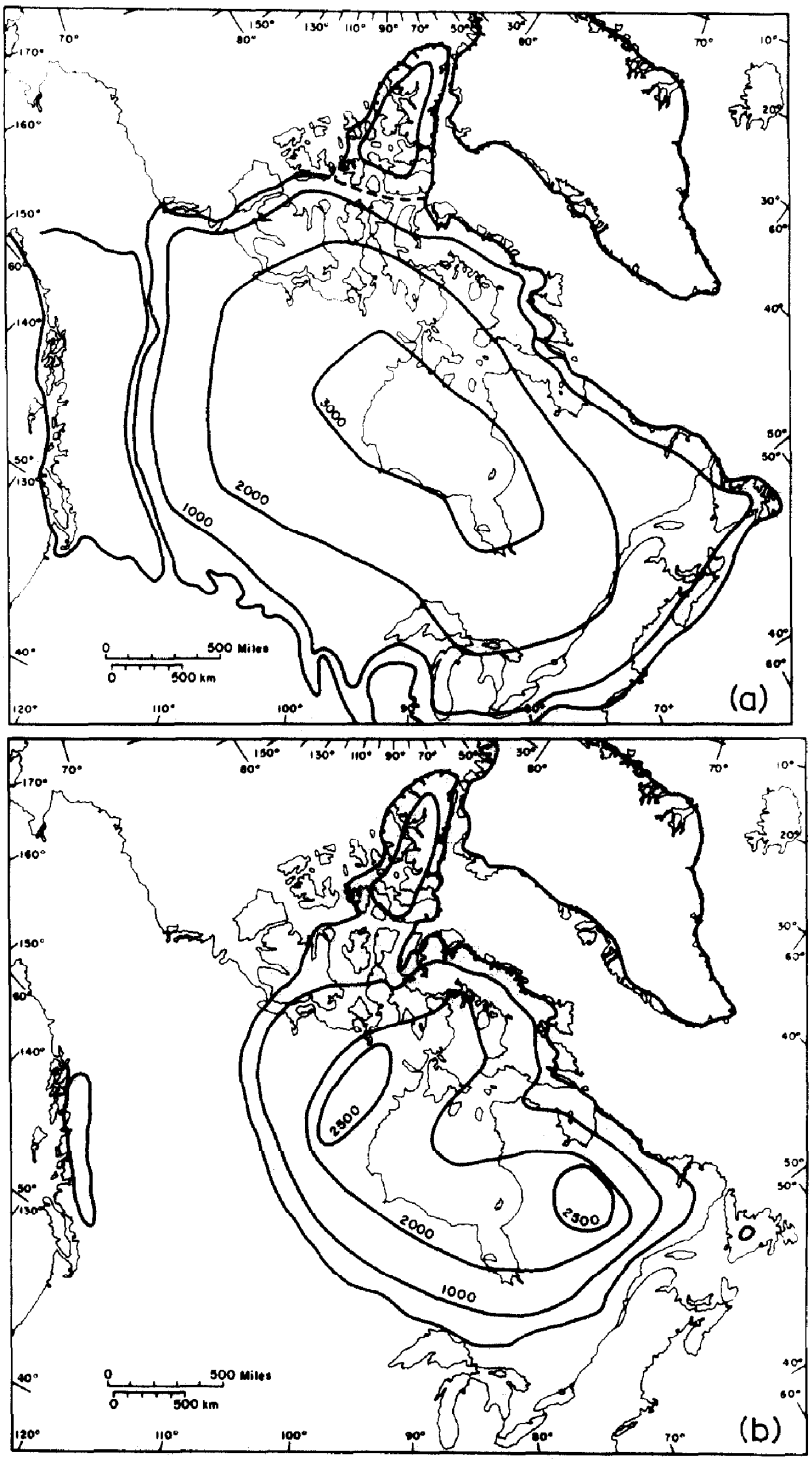

Fig. 5. The thickness of the Laurentide ice sheet in the model deglaciation history at two instants (a) Wisconsin maximum and (b) eight thousand years before present. Notice that the ice is assumed to retreat initially from over Hudson's Bay leaving high stands to the

the spatial distribution of M_O in the course of solving the problem. This will lead us to the Sea Level Equation which was described by Farrell and Clark (1976) and this will be discussed in the next section.

The second problem is associated with the determination of $L_I(\theta, \phi, t)$, the deglaciation chronology. In order to specify this function three distinct types of geological information are needed. We first assume that eq. 22 is correct to first order and as a measure of $S_{EUS}(t)$ we take relative sea level data from sites which are remote from the main centres of deglaciation. Such data indicate a net submergence which is on the order of 75—80 m since the last glacial maximum. Given $S_{EUS}(t)$ we compute $M_O(t)$ from eq. 22 then from mass conservation we get $M_I(t)$ directly. We next employ end moraine data which provide isochrons on the time dependent position of the edges of the major ice sheets. Knowing from this data the surface area of the major ice sheets as a function of time and the total mass which they must contain, the time dependent mass is partitioned among the major ice sheets in proportion to their instantaneous areas. Finally within each ice sheet and at each time we distribute the mass according to steady state ice mechanical arguments (Patterson, 1972) with allowance for other field data which make it possible to refine the distribution further. Such a "first guess" reconstruction of the major ice sheets (Fennoscandia and Laurentide) is tabulated in Peltier and Andrews (1976) and in Fig. 5a, b we show two time slices through the Laurentide ice history for 16 KBP and 8 KBP, respectively. In Fig. 6 we compare the corresponding $S_{EUS}(t)$ with the data described by

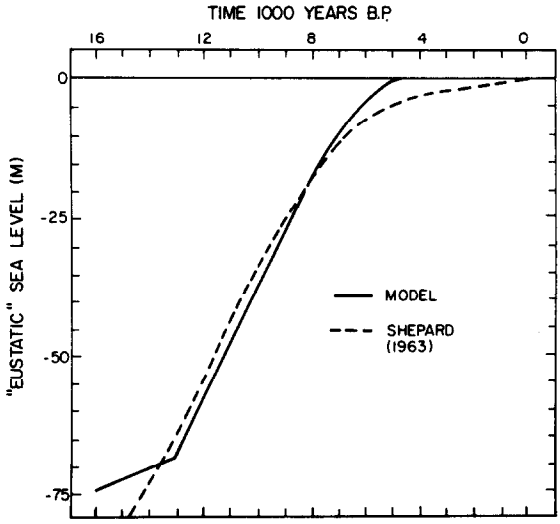

Fig. 6. The equivalent "eustatic" sea level curve for the deglaciation history tabulated in Peltier and Andrews (1976) compared to the observed eustatic curve of Shepard (1963). This constraint upon the deglaciation model is clearly satisfied.

Shepard (1963). Clearly our distintegration history fits this integral constraint quite accurately.

It must be emphasized that the ice sheet reconstruction described above is only approximate. The fact that we can make such a first guess, however, and one which we believe is reasonably accurate allows us to proceed with the solution of the forward problem. Given this deglaciation history we attempt to find, at first by guessing, the radial variation of viscosity which makes it possible to fit the observed relative sea level data. If we can find a viscosity profile which allows us to fit this data to some acceptable accuracy then we can proceed to refine *both* our knowledge of $M_I(\theta, \phi, t)$ *and* of $\nu(r)$ by employing the inverse theory outlined in Peltier (1976). The inverse problem is clearly non-linear because neither M_I nor $\nu(r)$ are known. We seek to deduce both directly from the relative sea level data by proceeding iteratively. We first fix M_I and refine ν; we then fix ν and refine M_I, continuing until (as we hope!) the process converges.

THE SEA LEVEL EQUATION

In the last section we left a major question unanswered and we turn to its resolution here. When the ice sheets melt and their meltwater is discharged to the ocean basins we must determine *where* in the oceans this water goes. This is clearly necessary if we wish to evaluate reponse integrals like eq. 18. Although we are able to obtain a reasonable a priori estimate for $L_I(\theta, \phi, t)$ as described in the last section we can as yet say little about $L_O(\theta, \phi, t)$ apart from the fact that it must conserve mass and thus satisfy the integral constraint eq. 22. By imposing the additional constraint that the surface of the ocean must be an equipotential surface at all times we may in fact deduce $L_O(\theta, \phi, t)$ *from* $L_I(\theta, \phi, t)$. Application of this constraint has led us (Farrell and Clark, 1976) to an explicit equation for the time variation of relative sea level locally. We review briefly the construction of this sea level equation in the remainder of this section.

Clearly the Green function for the forced variation of the gravitational potential must play a fundamental role in this discussion. We note that ϕ^H/g has the dimensions of length and begin by enquiring as to the meaning of this length scale. If we were to assume a single instant of melting then the net change of potential Φ at the earth's surface $r = a$ would be given by the convolution of ϕ^H with all mass loads as:

$$\Phi(\theta, \phi, t) = \rho_I \phi^H \underset{I}{*} L_I + \rho_W \phi^H \underset{O}{*} S \tag{23}$$

where the abbreviations $(\overset{*}{}_I)$ and $(\overset{*}{}_O)$ represent convolutions over the ice and oceans, respectively, and where we have replaced L_O by S, the local increase (decrease) of water thickness. The reason for this will become clear momentarily. The potential change Φ includes the effect due to the deformation of the surface of the planet since the function ϕ^H contains the Love number h_n.

This change in potential causes a change in the sea level with respect to the deformed surface of the solid earth in the amount (Farrell and Clark, 1976):

$$S = \frac{\Phi(\theta, \phi, t)}{g} + C \tag{24}$$

where the constant C is determined to ensure conservation of mass. Equation 24 is valid for sufficiently small changes S of the local bathymetry. It is important to note that S, by construction, is the local variation of sea level with respect to the surface of the solid earth and thus is precisely the relative sea level which one observes. Substituting eq. 24 into eq. 23 then gives:

$$S = \rho_I \frac{\phi^H}{g}_{*_I} L_I + \rho_W \frac{\phi^H}{g}_{*_O} S + C \tag{25}$$

To determine C we note that the integral over the surface area of the oceans of the product $\rho_W S$ must equal the instantaneous value of the total mass which has been lost by the ice sheets at time t. Thus:

$$\langle \rho_W S \rangle_O = \rho_W \left\langle \rho_I \frac{\phi^H}{g}_{*_I} L_I + \rho_W \frac{\phi^H}{g}_{*_O} S \right\rangle_O + \langle C \rangle_O \rho_W = -M_I(t) \tag{26}$$

The minus sign on the r.h.s. of eq. 26 is required since $M_I(t) < 0$ for load removal as discussed in the last section. Since C = constant thus $\langle C \rangle_O = CA_O$, thus:

$$C = -\frac{M_I(t)}{\rho_W A_O} - \frac{1}{A_O} \left\langle \rho_I \frac{\phi^H}{g}_{*_I} L_I + \rho_W \frac{\phi^H}{g}_{*_O} S \right\rangle_O \tag{27}$$

and in eqs. 26 and 27 we have used $\langle\ \rangle_O$ to indicate an integral over the surface area of the oceans.

With C given by eq. 27, eq. 25 is an integral equation for S which we call the sea level equation. It is an integral equation since S appears not only on the l.h.s. but also in the convolution integrals on the right. Given the deglaciation history $L_I(\theta, \phi, t)$ and thus $M_I(t)$ we may deduce the history of relative sea level $S(\theta, \phi, t)$ at any point on the surface (θ, ϕ) by inverting this integral equation.

In order to make the solution of eq. 25 practicable within the context of current (and foreseeable) limitations upon computing resources we are forced to discretize our description of the phenomenon both in time and in space. What we do in practice is to divide the "active" surface area of the earth into a number of finite elements which cover all of the ocean basins and that portion of the surface area of the continents at which actual deglaciation occurs. In addition we discretize the system in time and allow in the process for the fact that the deglaciation history and simultaneous ocean loading are not instantaneous. We assume that the mass load upon the finite element with

centroid at $\underline{r}'$ may be described by:

$$L(\underline{r}', t) = \sum_{l=1}^{P} L_l(\underline{r}')H(t - t_l) \tag{28}$$

where t_l ($l = 1, P$) are a series of times which bracket the entire loading history at $\underline{r}'$ and the $L_l(\underline{r}')$ are the loads applied or removed at the discrete times t_l. We allow the loads upon the "active" elements to change only at the times t_l and the times t_l are common to all active elements. This discrete approximation to the smooth functions $L(\underline{r}', t)$ may be made arbitrarily accurate by choosing a set of t_l with sufficiently small $\Delta t = t_{l+1} - t_l$. In practice we sample the deglaciation history and the response at a uniform $\Delta t = 10^3$ years.

With the above discrete specification of the load history in time we may write eq. 25 in the form:

$$S(\underline{r}, t) = \iint_{O} \rho_W S(\underline{r}', t) G^E(\underline{r} - \underline{r}')d\underline{r}' + \iint_{I} \rho_I I(\underline{r}', t) G^E(\underline{r} - \underline{r}')d\underline{r}'$$

$$+ \sum_{l=1}^{P} \iint_{O+I} L_l(\underline{r}')G^{HV}(\underline{r} - \underline{r}', t - t_l)d\underline{r}' - S_{EUS}(t) - K_C(t) \tag{29}$$

where we have expanded $\phi^H/g = G^E + G^{HV}$ into its elastic and viscous parts (Peltier, 1974; Peltier and Andrews, 1976) and the ice thickness has been represented simply as $L_I = I$. We note furthermore that in eqs. 28 and 29 L_l is a density weighted thickness. The function $S_{EUS}(t)$ corresponds to the first term in eq. 27, i.e.:

$$S_{EUS}(t) = \frac{\rho_I}{\rho_W A_O} \iint_{I} I(\underline{r}', t)d\underline{r}' \tag{30}$$

and $K_C(t)$ to the second term, i.e.:

$$K_C(t) = \frac{1}{A_O}\Big[\iint_{O} d\underline{r}'' \iint_{O} \rho_W G^E(\underline{r}'' - \underline{r}')S(\underline{r}', t)dr'$$

$$+ \iint_{O} d\underline{r}'' \iint_{I} \rho_I G^E(\underline{r}'' - \underline{r}')I(\underline{r}', t)dr'$$

$$+ \iint_{O} d\underline{r}'' \Big\{ \sum_{l=1}^{P} \iint_{O+I} L_l(\underline{r}')G^{HV}(\underline{r}'' - \underline{r}', t - t_l)d\underline{r}' \Big\}\Big] \tag{31}$$

In order to solve eq. 29 we proceed as mentioned above by splitting the entire active area of the surface into a number of discrete finite elements. The area of the j^{th} element we call E_j and on this area we assume that the load is piecewise constant in time. If $\underline{r}_i$ is the centroid of the i^{th} element

then the discrete version of eq. 29 is just:

$$a_{ip} = A_{ij}a_{jp} + B_{ij}b_{jp} + C_{iplj}c_{jl} - \frac{\rho_I}{\rho_W A_O} E_j b_{jp}$$

$$- \frac{1}{A_O}\left[E_i\{A_{ij}a_{jp} + B_{ij}b_{jp} + C_{iplj}c_{jl}\}\right] \tag{32}$$

in which a summation convention over repeated indices is implied such that $j = 1, N$ for terms involving a_{jp}; $j = N + 1, M$ for terms involving b_{jp}; $j = 1, M$ for terms involving c_{jl}; $l = 1, P_0$; $i = 1, N$. The upper limits in the summations are as follows:

N = the number of finite elements in the oceans
M = the total number of active elements (ocean plus ice)
P_0 = the number of time intervals ($\Delta t = 10^3$ years) since deglaciation commenced (33)

The lower case matrices are load dependent and are defined as follows:

$a_{ip} = S(\underline{r}_i, t_p)$, total relative sea level change at $\underline{r}_i$ for time t_p
$b_{ip} = I(\underline{r}_i, t_p)$, *total* thickness of ice removed from r_i by time t_p (34)
$c_{ip} = L_p(\underline{r}_i)$, incremental load change at $\underline{r}_i$ at time t_p

The upper case matrices depend only upon the geometry of the problem and the earth model. They are:

$$A_{ij} = \rho_W \iint_{E_j} G^E(\underline{r}_i - \underline{r}')d\underline{r}'$$

$$B_{ij} = \rho_I \iint_{E_j} G^E(\underline{r}_i - \underline{r}')d\underline{r}' = \frac{\rho_I}{\rho_W} A_{ij}$$

$$C_{iplj} = \iint_{E_j} G^{HV}(\underline{r}_i - \underline{r}', t_p - t_l)d\underline{r}' \tag{35}$$

In eq. 34 a_{ip} is an unknown matrix which is to be determined whereas b_{ip}, c_{ip} are input matrices which describe the deglaciation history.

The major computational expense in implementing the theory is connected with the calculation of the three "interaction matrices" A_{ij}, B_{ij}, C_{iplj}. These matrices depend only upon the geometric relations among the finite elements into which the "active" portion of the surface has been divided. In general, these interactions depend not only upon the separation between the field point $\underline{r}_i$ and the controid $\underline{r}_j$ of the element of area E_j and the magnitude of E_j, but also upon the *shape* of the element itself. In the interest of efficiency we have elected initially to suppress this shape dependence and to replace each finite element by a circular disk of equivalent area in calculating the matrix components. This assumption may of course be

relaxed. We construct a table of disc factors as described by Farrell (1973) for an equivalent elastic problem and by Peltier and Andrews (1976) for the visco-elastic system. The normalization of the elements of this table is however different from that employed in these papers. For the visco-elastic problem the necessity of this was pointed out by Peltier and Andrews (1976). The new normalization factor is essentially the square of the angular separation between the field point and the centre of the disc (Clark, 1977). Linear interpolation in a regular table of disc factors is then employed to deduce the matrix components.

Given these geometry and earth model dependent matrices and the matrix specification of the deglaciation history we solve eq. 32 at each point in time by applying conventional relaxation methods. At each time t_p we make a first guess to the matrix a_{ip} and substitute this into eq. 32 to compute the residual. This residual is then fed back to update the first estimate and the process is continued until convergence is achieved. In practice three such iterations are normally sufficient (Farrell and Clark, 1976).

INITIAL RESULTS

Here we will discuss the results of applying the discrete form of the sea level eq. 32 in an initial series of calculations. These results have all been described elsewhere (Clark, 1978; Clark et al., 1978; Peltier, 1978) and the interested reader is referred to these articles for a more detailed discussion. The earth model employed is the first for which Green functions were derived in Peltier (1974) and later subjected to preliminary test in Peltier and Andrews (1976). It has an elastic structure which is Gutenburg-Bullen "A", an inviscid core and no lithosphere. Throughout the mantle the viscosity has a constant value of 10^{22} poise (cgs). It is the model which Cathles (1975) and Peltier and Andrews (1976) have claimed provides a good fit to a wide range of relative sea level data although this conclusion was in both cases based upon calculations which were not gravitationally self-consistent. The glacial history employed is that tabulated in Peltier and Andrews (1976) although this was refined somewhat by linear interpolation to give ice thickness at each active point at equispaced times separated by $\Delta t = 10^3$ years. This deglaciation history gives the equivalent "eustatic" sea level curve previously shown in Fig. 6.

The first output from the calculation is the global prediction of the relative sea level variation since the initiation of melting. It is *assumed* that the major ice sheets were in isostatic equilibrium before retreat commenced. Four time slices through the global solution are shown in Fig. 7. The sea level rise (fall) is contoured in metres. Clearly the rise of sea level in the "far field" of the ice sheets is not uniform as must be the case if the surface of the new ocean is to remain equipotential. The large fall of sea level relative to the surface of the solid earth in regions which were once ice covered (Fennoscandia, Laurentide) is also clearly evident. From this output we may

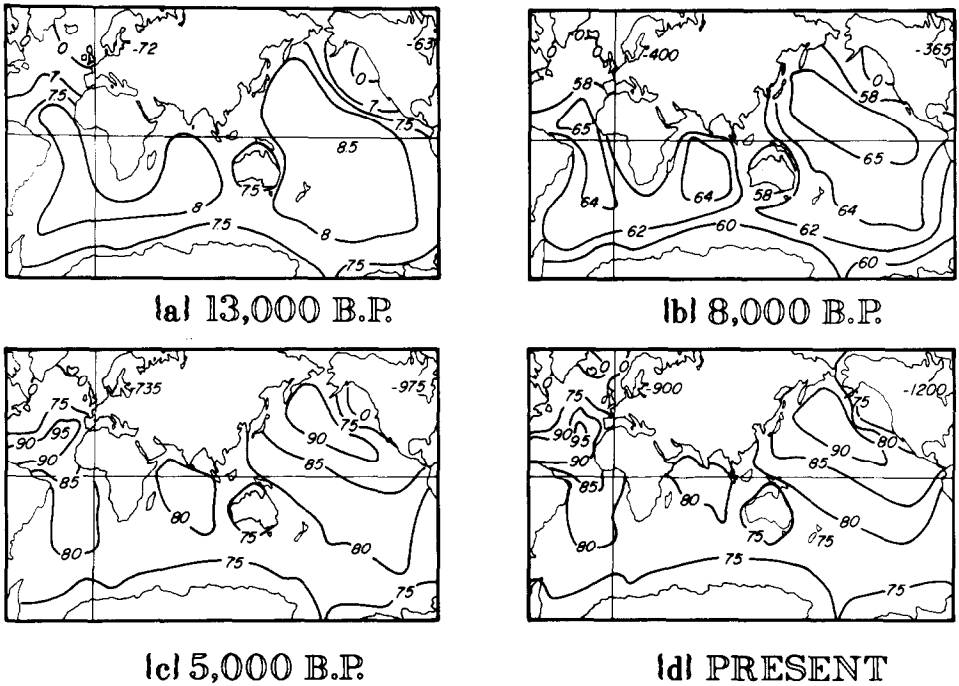

Fig. 7. The global rise of sea level (in metres) at four times subsequent to the onset of melting. Note the large negative values corresponding to a fall of local sea level in the vicinity of the Laurentide and Fennoscandia ice sheets. The rise of sea level is not uniform in the far field showing explicitly that the concept of eustatic sea level is of limited utility.

directly deduce relative sea level for any point on the surface for which we have observations available. Inspection of a complete set of output data (Clark et al., 1978) reveals that the surface may be divided roughly into six major regions within which there exists a fairly unique relative sea level signature. These regions are shown in Fig. 8 and their characteristics are as follows.

In I there is continuous emergence following deglaciation and these regions are those which were once under the ice sheets. In II there is continuous submergence due to the collapse of the proglacial forebulge (Peltier, 1974). In addition there is a rather narrow region separating I and II in which the relative sea level history is not monotonic, initial emergence is followed by submergence. This effect is due to the migration of the forebulge inwards (Peltier, 1974). In region III there is slight time dependent emergence and this occurs only over a very limited area of the globe (Clark et al., 1978). In IV there is continuous oceanic submergence and in V there is emergence which begins immediately upon the cessation of melting (Clark et al., 1978). Region VI consists of all continental shorelines which are sufficiently remote from the main deglaciation centres. Such locations are char-

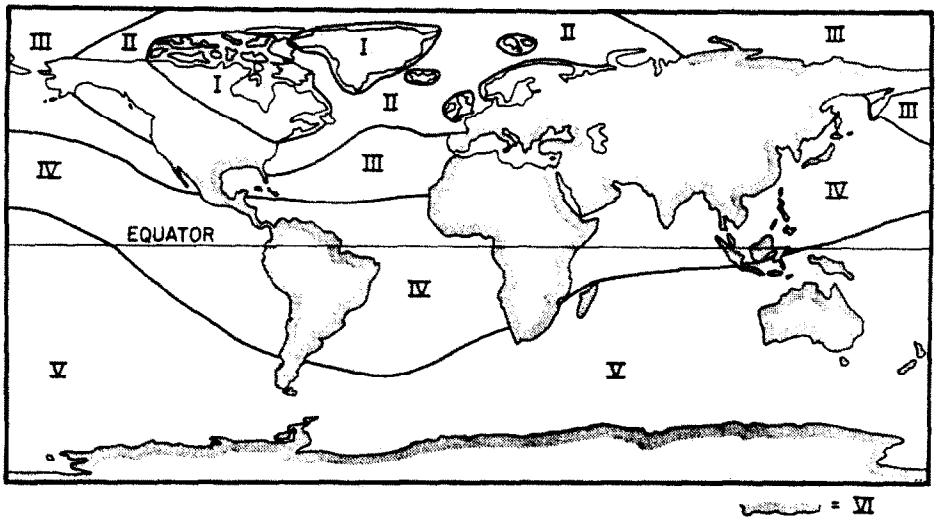

Fig. 8. The global extent of regions I—VI in each of which the sea level curve has a certain characteristic signature. The characteristics of this signature are described in the text.

acterized by emergence due to crustal tilting which is forced by the adjacent water load (Walcott, 1972). In the following paragraphs we compare briefly the predictions of the model with observed relative sea level data in each of these regions. The sources of the data shown on the following figures are listed in abbreviated form as an appendix to the main bibliography.

Figure 9 shows observations in region I respectively for the Laurentide (Ottawa Islands) and Fennoscandia (Oslo Fjord) regions and the superimposed predictions of the model for the two sites. At the former location the prediction is considerably in excess of the observed emergence indicating

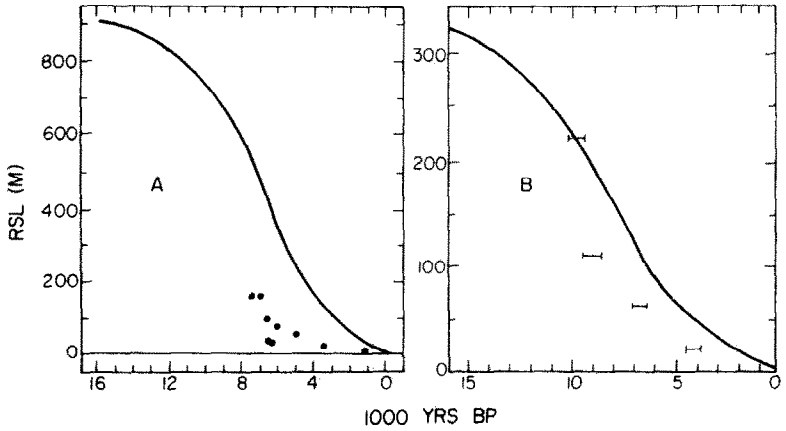

Fig. 9. Comparison of theory and observation for two sites in region I. A. Ottawa Islands, Hudson's Bay. B. Oslo Fjord, Norway.

either that the load removed over Hudson's Bay was somewhat large or that the rheology is incorrect or both. The fit to the data at the Oslo Fjord site is much better although the amount of emergence predicted is again somewhat in excess of the observation.

In Fig. 10 we compare theory with observation at a sequence of locations extending southward along the eastern seaboard of the continental U.S. in region II (Clark et al., 1978). Although continuous submergence is observed and predicted the model calculation gives excessive submergence, the error of fit being on the order of 100% for some sites. This again suggests that the load removed may have been too large or that the earth model is in error. In Fig. 11 the prediction is compared to observation at an equivalent location with respect to the Fennoscandia ice sheet, namely along the Atlantic coast of France. The dashed curve is for northern France (region II) and the solid curve for southern France (region III). All of the data along the French coast should lie between these two extremes and the gross error of fit is seen to be small (Clark, 1978).

In Fig. 12 we compare theory and observation at a sequence of locations near the edge of the ice sheet for the Cumberland Peninsula on Baffin Island (Canada). This comparison is from Clark (1978) and illustrates the characteristic non-monotonic nature of the relative sea level curves from such regions which was predicted by Peltier (1974) by direct inspection of the Green

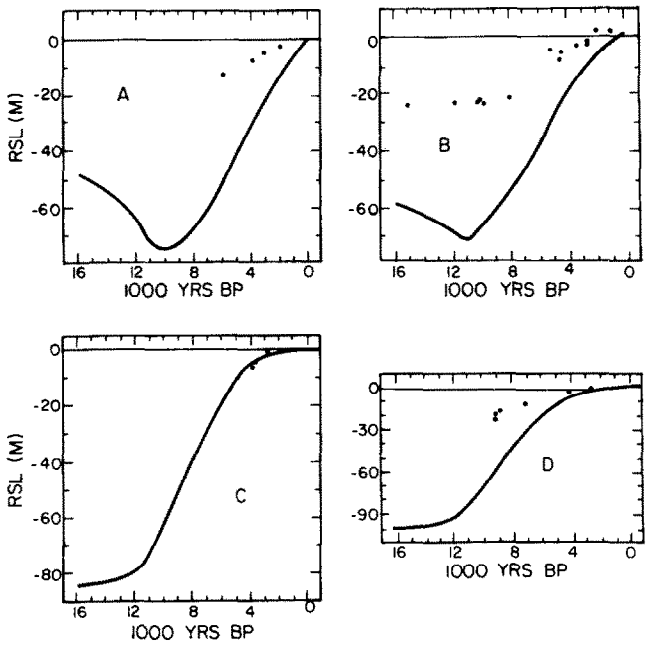

Fig. 10. Comparison of theory and observation for four sites along the eastern seaboard of the U.S. in region II. A. Brigantine, New Jersey. B. Virginia. C. Georgia. D. Bermuda.

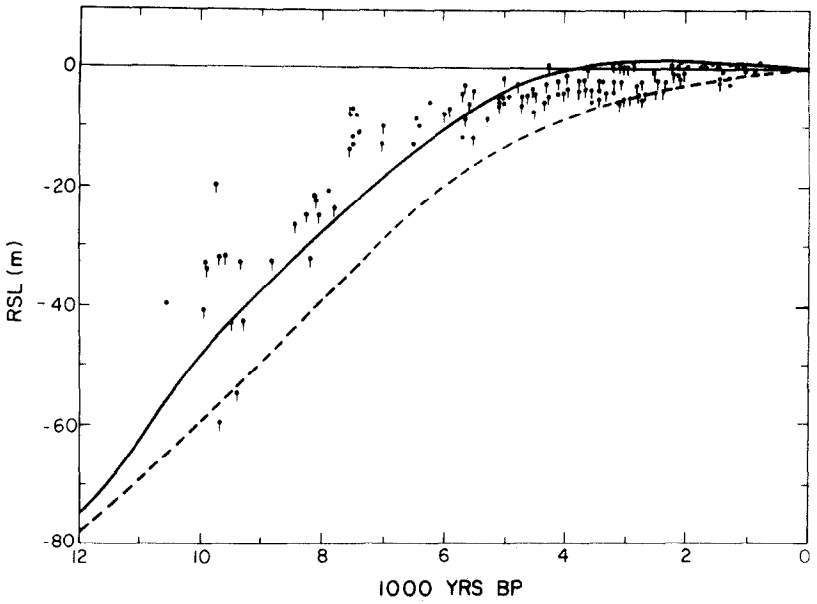

Fig. 11. Comparison of theory and observation for a segment of region II along the Atlantic coast of France. The solid curve is the prediction for sites in southern France (region III) while the dashed curve is for northern France (region II). The data from the French coast are seen to be bounded by these extremes.

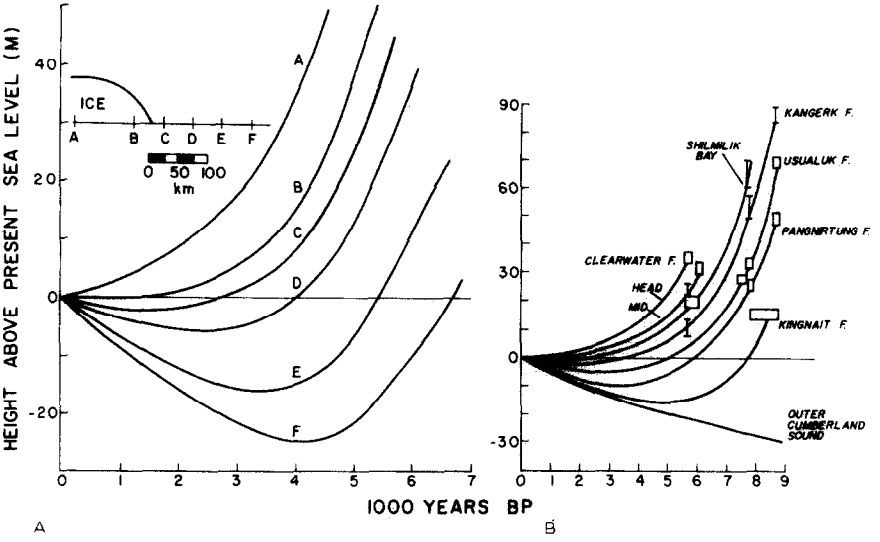

Fig. 12. Comparison of theory (A) with observations (B) at a sequence of sites near the edge of the ice sheet on the Cumberland peninsula of Baffin Island (boundary between region I and region II).

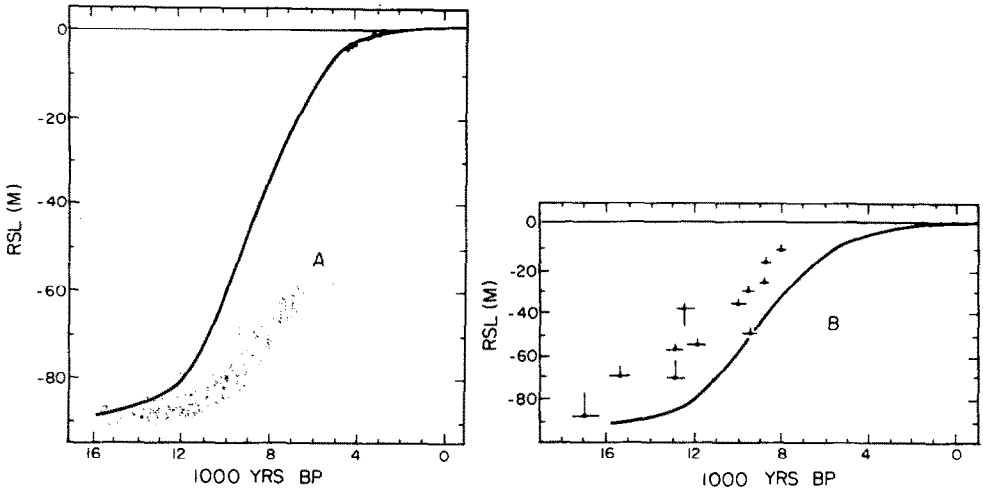

Fig. 13. Comparison of theory and observation at two sites in region III: (A) Florida, (B) Gulf of Mexico.

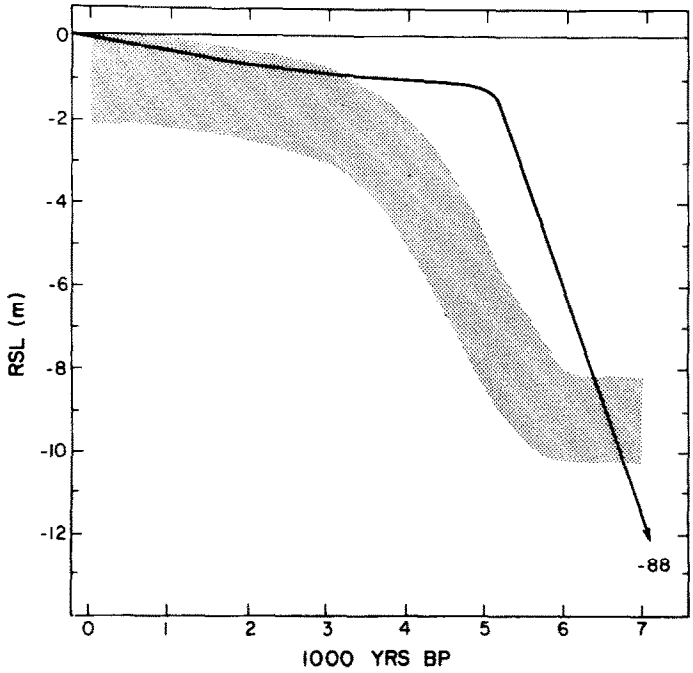

Fig. 14. An example of theory vs. observation at a site in region IV. This is for Oahu, Hawaii. The large divergence near $6 \cdot 10^3$ years before present is presumed to be associated with the volcanic eruption which took place at that time and is thus associated with local tectonics.

functions for the present earth model. Such sites are found on the boundary between regions I and II.

Examples of the comparison between theory and observation in region III are shown in Fig. 13 respectively for Florida and for the Gulf of Mexico. For the latter location the sea level record is extremely long and for both the fit of the theory to the observations is rather good. These comparisons were described previously in Clark et al. (1978) and some additional discussion is found in Peltier (1978).

As an example from region IV we show the comparison of theory and observation for Oahu, Hawaii (from Clark, 1978) in Fig. 14. Here again the magnitude of the misfit is acceptably small, the largest deviation occurring at roughly five thousand years before the present at the time of the last major volcanic eruption and therefore presumably due to local tectonics. In Fig. 15 (Clark, 1978) the relative sea level data from New Zealand (region V) is compared to the theoretical calculation. Here again the error of fit is observed to be small. Finally in Fig. 16 (Clark et al., 1978) we compare with theory the observations at a site in region VI. These data are for Recife, Brazil and illustrate the characteristic emergence at continental shorelines in the far field. The solid curve is the prediction for the coastline and the dashed curve for a site on the continental shelf 100 km east of Recife. The latter shows contin-

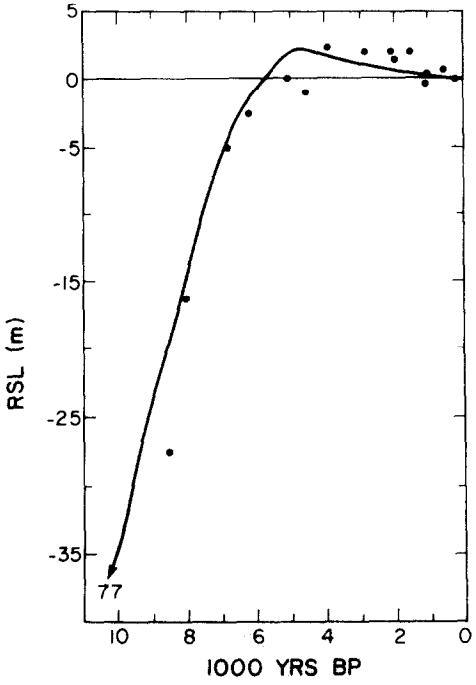

Fig. 15. Comparison of theory and observation for a site in region V. This is for New Zealand. The point is that even in the far field the fit to the observations is rather good.

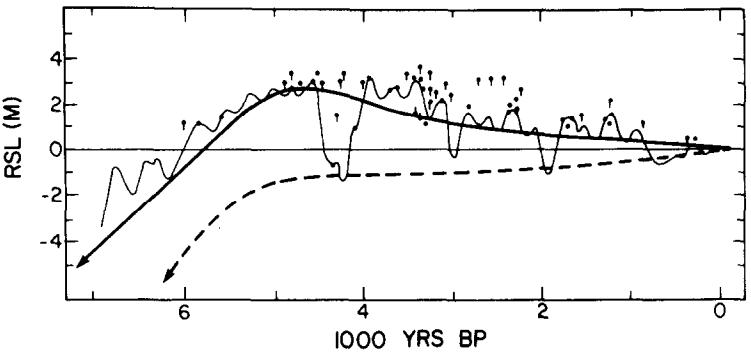

Fig. 16. Comparison of theory and observation for a site (Recife, Brazil) in region VI. This illustrates the characteristic emergence due to crustal tilting along continental margins in the far field.

uous submergence characteristic of region IV. The Fairbridge curve (light line) is bracketed by these two predictions.

DISCUSSION AND SUMMARY

The comparison of theory and observation detailed in the last section is encouraging in that it has provided a positive test of both the rheology model and of the deglaciation history. As is clear from the way in which the theory has been constructed, the problem of glacial isostatic adjustment is highly non-linear in that the observed response (relative sea level data) is dependent both upon the rheology and upon the deglaciation history. If we are to discover *a* viscosity profile and *an* unloading history which are unique in the sense of being known within limits prescribed by our knowledge of the data then we must be able to perform an initial linearization of the problem with some confidence. We have done this by employing a "first guess" deglaciation history which is in accord with the best information currently available from Quaternary geology. That this first guess load history and a first guess viscosity profile (also conditioned by a priori knowledge) have led to substantial accord with the observations convinces us that we may proceed with the iterative refinement of both functionals in the manner outlined in Peltier (1976) and the refinement of $I(\theta, \phi, t)$ has already begun (Clark, 1977).

There remain certain characteristic misfits between theory and observation which will provide guidance as we proceed with this work. Most notably, the relative sea level data for the Laurentide region show rather large departures from theory *in the near field.* Although we expect that the incorporation of a lithosphere into the model (Peltier, 1978) may remedy some of the defects it is rather unlikely, indeed impossible, that the major errors are derivative of this source. Either the earth model is more fundamentally in error or the load history is incorrect. Because the large errors of fit are con-

fined to the Laurentide region and do not exist in the vicinity of Fennoscandia we suspect that the latter is more likely to be the case. These questions are under current consideration.

Because these characteristic misfits still remain in the near field of the Laurentide ice sheet we are as yet not able to confirm or to deny with complete confidence the conclusions previously drawn by Cathles (1975) and by Peltier and Andrews (1976). If "fine tuning" of these calculations does reconfirm these conclusions (as we suspect will be the case), namely that within the context of a Newtonian viscous rheology the viscosity of the mantle *must be* essentially constant in order to fit the rebound data, then the implications for mantle convection are important. Peltier (1972) has shown that the mixing length for convection in the mantle would then be on the order of the mantle thickness itself.

Aside from determining *a* mantle viscosity profile which allows us to fit the data we would also like to know the envelope of viscosity profiles which are capable of satisfying all of the data to within a standard error. This quantification of the extent to which the rebound information allows us to remain ignorant is perhaps the most important information which we could extract from the point of view of the solid state theory of microphysical creep mechanisms.

Here we have described only the constraints upon a Newtonian rheology which are implied by the relative sea level data themselves. There are at least two further observational data which are also capable of providing important information. The first of these, and perhaps the most important, are data concerning the present day gravity anomalies over the rebound centres. These data are particularly important because they provide information which is completely distinct from that afforded by the relative sea level data. Gravity data, in a real sense, "looks into the future" because such data essentially measure the degree of current gravitational disequilibrium and are therefore indicative of the amount of uplift (subsidence) remaining which is well known. The gravity data therefore "see" the long time tail of the relaxation spectrum whereas the sea level data do not. In order to predict the gravity anomaly with the present theory we *require* a model with a lithosphere (Peltier, 1978).

Besides the gravity data we may also expect to obtain interesting (although perhaps not so immediately useful) information by analysis of the non-tidal deceleration of rotation which is forced by the deglaciation event. The large shift in surface mass is clearly sufficient to produce a relatively large change in the components of the inertia tensor and thus a change in the length of the day. Although interesting in itself and in providing an additional constraint on deep mantle viscosity (O'Connell, 1971) this effect may be most interesting from a climatological point of view. It should be clear that there remains a significant amount of work to be done before we may properly claim a complete understanding of the phenomenon of glacial isostasy.

REFERENCES

Ashby, M.F., 1972. A first report on deformation mechanism maps. Acta Metall., 20: 887.

Biot, M.A., 1954. Theory of stress-strain relations in anisotropic visco-elasticity and relaxation phenomena. J. Appl. Phys., 25 (11): 1385.

Brennan, C., 1974. Isostatic recovery and the strain rate dependent viscosity of the earth's mantle. J. Geophys. Res., 79: 3993.

Cathles, L.M., 1975. The Viscosity of the Earth's Mantle. Princeton University Press, Princeton, New Jersey, 386 pp.

Clark, J.A., 1977. Global Sea Level Changes Since the Last Glacial Maximum. Thesis, Dept. of Geol. Sciences, University of Colorado, Boulder, Colo. (unpublished).

Clark, J.A., 1978. A numerical model of worldwide sea level changes on a visco-elastic earth. Proceedings of the Stockholm Conference on Earth Rheology and Late Cenozoic Vertical Movements (in press).

Clark, J.A., Farrell, W.E. and Peltier, W.R., 1978. Global changes in postglacial sea level: a numerical calculation. Quat. Res. (N.Y.), (in press).

Crough, S.T., 1977. Isostatic rebound and power law flow in the asthenosphere. Geophys. J. R. Astron. Soc., 50: 723.

Farrell, W.E., 1972. Deformation of the earth by surface loads. Rev. Geophys. Space Phys., 10: 761.

Farrell, W.E., 1973. Earth tides, ocean tides, and tidal loading. Phil. Trans. R. Soc. London, Ser. A, 274: 45.

Farrell, W.E. and Clark, J.A., 1976. On postglacial sea level. Geophys. J. R. Astron. Soc., 46: 647.

Goldreich, P. and Toomre, A., 1969. Some remarks on polar wandering. J. Geophys. Res., 74: 2555.

Haskell, N.A., 1935. The motion of a viscous fluid under a surface load. Physics, 6: 265.

Haskell, N.A., 1936. The motion of a viscous fluid under a surface load, 2. Physics, 7, 56:

Haskell, N.A., 1937. The viscosity of the asthenosphere. Am. J. Sci., 33: 22.

Herring, C., 1950. Diffusional viscosity of a polycrystalline solid. J. Appl. Phys., 21: 437.

Isacks, B. and Molnar, P., 1971. Distribution of stresses in the descending lithosphere from a global survey of focal mechanism solutions of mantle earthquakes. Rev. Geophys. Space Phys., 9: 103.

Kanamori, H. and Anderson, D.L., 1977. Importance of physical dispersion in surface wave and free oscillation problems: Review. Rev. Geophys. Space Phys., 15 (11): 105.

Kohlstedt, D. and Goetze, C., 1974. Low-stress high-temperature creep in olivine single crystals. J. Geophys. Res., 79: 2045.

Lee, E.H., 1955. Stress analysis in visco-elastic bodies. Q. Appl. Math., 13: 183.

Libby, W.F., 1952. Radiocarbon Dating. The University of Chicago Press, Chicago and London.

Liu, H.P., Anderson, D.L. and Kanamori, H., 1976. Velocity dispersion due to anelasticity: Implications for seismology and mantle composition. Geophys. J. R. Astron. Soc., 47: 41.

Love, A.E.H., 1967 (1911). Some Problems of Geodynamics. Dover Publications Inc., New York, 180 pp.

Malvern, L.E., 1969. Introduction to the Mechanics of a Continuous Medium. Prentice-Hall Inc., Englewood Cliffs, N.J.

McConnell, R.K., 1968. Viscosity of the mantle from relaxation time spectra of isostatic adjustment. J. Geophys. Res., 73: 7089.

McKenzie, D.P., 1966. The viscosity of the lower mantle. J. Geophys. Res., 71: 3995.

Munk, W.H. and MacDonald, G.J.F., 1960. The Rotation of the Earth. Cambridge University Press, Cambridge, Mass.

Niskanen, E., 1948. On the viscosity of the earth's interior and crust. Ann. Acad. Sci. Fenn., Ser. A3 (15): 22.
O'Connell, R.J., 1971. Pleistocene glaciation and the viscosity of the lower mantle. Geophys. J. R. Astron. Soc., 23: 299.
Parsons, B.E., 1972. Changes in the Earth's Shape. Thesis, Cambridge Univ., Cambridge (G.B.).
Patterson, W.S.B., 1972. Laurentide ice sheet: Estimated volumes during late Wisconsin. Rev. Geophys. Space Phys., 10: 885.
Peltier, W.R., 1972. Penetrative convection in the planetary mantle. Geophys. Fluid Dyn., 5: 47.
Peltier, W.R., 1974. The impulse response of a Maxwell earth. Rev. Geophys. Space Phys., 12 (4): 649.
Peltier, W.R., 1976. Glacial isostatic adjustment — II: The inverse problem. Geophys. J. R. Astron. Soc., 46: 669.
Peltier, W.R., 1978. Ice sheets, oceans, and the earth's shape. Proceedings of the Stockholm Conference on Earth Rheology and Late Cenozoic Movements (in press).
Peltier, W.R. and Andrews, J.T., 1976. Glacial isostatic adjustment — I: The forward problem. Geophys. J. R. Astron. Soc., 46: 605.
Post, R. and Griggs, D., 1973. The earth's mantle: evidence of non-Newtonian flow. Science, 181: 1242.
Sammis, C.G., Smith, J.C., Schubert, G. and Yuen, D.A., 1977. Viscosity-depth profile of the earth's mantle: effects of polymorphic phase transitions. J. Geophys. Res., 82: 3747.
Shepard, F.P., 1963. 35,000 years of sea level. In: Essays in Marine Geology. Univ. Southern California Press, 1.
Stocker, R.L. and Ashby, M.F., 1973. On the rheology of the upper mantle. Rev. Geophys. Space Phys., 11: 391.
Vening Meinesz, F.A., 1937. The determination of the earth's plasticity from post glacial uplift of Scandinavia: isostatic adjustment. Proc. K. Ned. Akad. Wet., 40: 654.
Walcott, R.I., 1972. Late Quaternary vertical movements in eastern North America: Quantitative evidence of glacio-isostatic rebound. Rev. Geophys. Space Phys., 10: 849.
Weertman, J. and Weertman, J.R., 1975. High temperature creep of rock and mantle viscosity. A. Rev. Earth Planet. Sci., 3: 293.

SEA LEVEL DATA SOURCES

Fig. 9A. Andrews, J.T. and Falconer, G., 1969. Can. J. Earth Sci., 6: 1263—1276.
Fig. 9B. In: T.C. Kenney, 1964. Geotechnique, 14: 203—230.
Fig. 10A. Stuiver, M. and Deddario, H.J., 1963. Science, 142: 951.
Fig. 10B. Harrison, W., Malby, R.J., Rusnak, G.A. and Terasmee, J., 1965. J. Glaciol., 73: 201—229.
Newman, W.S. and Rusnak, G.A., 1965. Science, 148: 1464—1466.
Fig. 10C. Wait, R.L., 1968. U.S. Geol. Surv., Prof. Pap., 600-D: 38—41.
Fig. 10D. Newman, A.C., 1971. Quaternaria, 14: 41—43.
Fig. 11. Ters, M., 1973. Assoc. Fr. Étude Quat., Suppl. au Bull., 36: 114—142.
Fig. 12B. Dyke, A., 1977. Unpublished Ph.D. Thesis, Univ. of Colorado, Dept. of Geography, Boulder, Colorado, 184 pp.
Fig. 13A. Scholl, D.W. and Stuiver, M., 1967. Geol. Soc. Am. Bull., 78: 437—454.
Fig. 13B. Curray, J.R., 1960. In: Recent Sediments N.W. Gulf of Mexico. Am. Assoc. Pet. Geol., pp. 221—266.
Fig. 14. Easton, W.H. and Olson, E.A., 1976. Geol. Soc. Am. Bull., 87: 711—719.
Fig. 15. Schofield, J.C., 1964. N.Z. J. Geol. Geophys., 7: 359—370.
Fig. 16. Fairbridge, R.W., 1976. Science, 191: 353—359.